



Cite this: *Chem. Commun.*, 2016, 52, 2122

Received 13th November 2015,  
Accepted 4th December 2015

DOI: 10.1039/c5cc09409g

www.rsc.org/chemcomm

# Detection of quadrupolar nuclei by ultrafast 2D NMR: exploring the case of deuterated analytes aligned in chiral oriented solvents†

Philippe Lesot,<sup>\*ab</sup> Philippe Berdagué<sup>a</sup> and Patrick Giraudeau<sup>\*cd</sup>

**Anisotropic <sup>2</sup>H ultrafast (ADUF) 2D NMR spectroscopy for studying analytes dissolved in chiral liquid crystals (CLC) is investigated for the first time and the analytical possibilities of this method are evaluated. We demonstrate that these unconventional sub-second 2D experiments are compatible with the basic gradient units (40–60 G cm<sup>-1</sup>) that are implemented in routine spectrometers and allow the recording of <sup>2</sup>H signals of weakly aligned deuterated solutes in sub-second experimental times.**

A major advantage of proton-decoupled deuterium (<sup>2</sup>H-{<sup>1</sup>H}) nD NMR spectroscopy in oriented media such as liquid crystals (LCs) is the access to anisotropic spectral data that are averaged to zero in liquids, such as chemical shift anisotropy (<sup>2</sup>H CSA) and residual quadrupolar coupling (denoted as RQC(<sup>2</sup>H) or Δν<sub>Q</sub>(<sup>2</sup>H)). These order-dependent data can provide key information on the molecular geometry, conformational behavior and dynamics of aligned analytes (solutes or mesophases themselves).<sup>1</sup>

Compared with other nuclei with  $I > 1/2$ , deuterons possess a small quadrupolar moment ( $Q_D = 2.86 \times 10^{-31} \text{ m}^2$ ),<sup>2</sup> which thus limits excessive line broadening owing to quadrupolar relaxation mechanisms. When dissolved in rather weakly oriented LCs such as lyotropic polypeptide systems, they produce <sup>2</sup>H quadrupolar doublets (QD), whose magnitude of |Δν<sub>Q</sub>| generally ranges from 0 to 1000 Hz. Interestingly, because these aligning media are chiral (helical polymers), the spectral enantiodiscrimination of the enantiotopic directions of deuterated prochiral molecules or enantiomers is possible on the basis of a difference in RQC ( $\Delta\nu_Q(^2\text{H})^R \text{ or pro-}R \neq \Delta\nu_Q(^2\text{H})^S \text{ or pro-}S$ ).<sup>3</sup>

Based on this strategy, various methodological developments (<sup>2</sup>H nD NMR) and a large range of applications (stereochemical analysis) have been proposed, including the detection of deuterium at natural abundance levels (isotope fractionation analysis).<sup>4</sup>

Very recently, the first monitoring of chiral enzymatic transformations (the interconversion of L- and D-alanine-d<sub>3</sub> enantiomers by alanine racemase) directly observed by anisotropic <sup>2</sup>H NMR has been successfully pioneered.<sup>5</sup> The idea was to follow *in situ* and in real time the variation in the peak intensity of the QDs of each enantiomer during the bioprocess and determine from the spectral fit the turnover numbers of the enzyme. An inherent drawback of this approach is the experimental time that is required to record spectral data for monitoring the time-dependent variations of all compounds in the mixture, in particular for extremely fast and/or multiple (cascade) chemical transformations in which the fast identification and quantification of <sup>2</sup>H signals of products (reactants, (un)stable intermediates, products, *etc.*) (whether chiral or not) require 2D NMR experiments with sub-minute time resolutions or below.

Non-uniform acquisitions combined with covariance/compressed sensing processing<sup>6</sup> have been proposed to reduce the acquisition time in anisotropic NAD 2D NMR experiments. Another appealing option is to rely on ultrafast (UF) 2D NMR, which is an approach capable of yielding homo- or heteronuclear 2D correlations within a single scan when its sensitivity allows this.<sup>7</sup> Within the last ten years, the performance of UF experiments has been greatly enhanced by numerous methodological developments, which make UF NMR applicable to a wide range of analytical situations.<sup>8</sup> UF NMR has been applied to the real-time monitoring of fast chemical transformations,<sup>9</sup> the coupling with other techniques such as chromatography<sup>10</sup> or hyperpolarization,<sup>11</sup> and also the high-throughput quantitative analysis of complex samples.<sup>12</sup>

The use of UF 2D NMR experiments in anisotropic environments was described in 2012<sup>13</sup> for determining residual <sup>13</sup>C-<sup>1</sup>H dipolar couplings (RDC's) from UF heteronuclear spectra. However, such an approach has never been investigated in the case of quadrupolar nuclei such as deuterium ( $I = 1$ ) using aligned solvents.

In this communication, we report the first examples of anisotropic deuterium UF (ADUF) spectra of deuterated analytes

<sup>a</sup> Equipe RMN en Milieu Orienté, ICMO, UMR-CNRS 8182, Université de Paris-Sud, Université Paris-Saclay, Rue du Doyen Georges Poitou, Bât. 410, 91405 Orsay cedex, France. E-mail: philippe.lesot@u-psud.fr

<sup>b</sup> CNRS/INC, 3 rue Michel Ange, 75016 Paris, France

<sup>c</sup> Equipe EBSI, CEISAM, UMR-CNRS 6230, Université de Nantes, 2, Chemin de la Houssinière, 44300 Nantes, France. E-mail: patrick.giraudeau@univ-nantes.fr

<sup>d</sup> Institut Universitaire de France, 1 rue Descartes, 75005 Paris Cedex 05, France

† Electronic supplementary information (ESI) available: Anisotropic <sup>2</sup>H 1D and 2D conventional spectra of **1** and **2**. See DOI: 10.1039/c5cc09409g



dissolved in lyotropic polypeptide CLCs. We investigate the cases of two isotopically enriched prochiral molecules of  $C_s$  symmetry on average, pentanol- $d_{12}$  (**1**) and benzyl alcohol (**2**) enriched in  $^{13}\text{C}$  and  $^2\text{H}$  on the prostereogenic methylene group, both of which possess enantiotopic C–D directions. Although these prochiral molecules possess rather few inequivalent  $^2\text{H}$  sites (see Fig. 2 and 3), they represent interesting model compounds for discussing the analytical possibilities of ADUF 2D NMR in CLCs and also for investigating the case of spectrally detectable isotopologues.

The ADUF 2D pulse sequence shown in Fig. 1 follows the basic scheme of homonuclear UF 2D experiments, where the usual time encoding is replaced by spatial encoding, which is formed by two chirp pulses applied together with a pair of opposite gradients.<sup>14</sup> This spatial encoding block is followed by a conventional mixing period and a detection block based on echo planar spectroscopic imaging (EPSI).<sup>15</sup> The  $^2\text{H}$  hard-pulse scheme is identical to the Q-COSY sequence that was developed for conventional  $^2\text{H}$  experiments (QUOSY-type) and generates magnitude-mode maps.<sup>2,3,16</sup> It comprises a  $^2\text{H}$   $90^\circ(x)$  pulse followed by a  $180^\circ(x)$  pulse, separated by a spatial encoding period of duration TE. In contrast to conventional 2D Q-COSY experiments, the ADUF 2D scheme is a constant-time experiment, which leads to the refocusing of all coupling patterns in the  $F_2$  dimension. Note that in all UF experiments shown here the spatially-encoded dimension is shown in  $F_2$ , whereas the dimension

that results from a Fourier transform of the EPSI domain is shown in  $F_1$ . In the case of  $^2\text{H}$  nuclei, the former consists of removing all  $\Delta\nu_Q(^2\text{H})$  in the  $F_2$  dimension of the 2D map, together with the possible homonuclear scalar  $^nJ(^2\text{H}-^2\text{H})$  and dipolar  $^nD(^2\text{H}-^2\text{H})$  couplings in the case of perdeuterated molecules. In other words, the expected ADUF 2D map is formally identical to that obtained for conventional  $\delta$ -resolved experiments (QUOSY-type), except that the spectral contents of  $F_1$  and  $F_2$  are inverted compared with conventional spectra<sup>16</sup> (see ESI†). Consequently, ADUF experiments can be considered as  $^2\text{H}$   $\delta$ -resolved constant-time experiments.

Possible  $^nJ(^2\text{H}-^1\text{H})$  and  $^nD(^2\text{H}-^1\text{H})$  heteronuclear couplings (which are generally  $< 2$  Hz in a PBLG mesophase) can be simply removed by implementing  $^1\text{H}$   $180^\circ$  hard pulses between the bipolar gradient pairs, in order to refocus such couplings during the spatial encoding and/or acquisition periods. These pairs of  $180^\circ$  pulses can also be associated with similar pulses on the heteronuclear X channel for further X– $^2\text{H}$  heteronuclear decoupling. Fig. 1 shows such an optional block for specific decoupling of  $^{13}\text{C}$ . Note that owing to the smaller gyromagnetic value of  $^2\text{H}$  nuclei compared with  $^1\text{H}$  ( $\gamma_{^1\text{H}} = 6.515 \times \gamma_{^2\text{H}}$ ), the magnitude of  $^nJ(^2\text{H}-^{13}\text{C})$  and  $^nD(^2\text{H}-^{13}\text{C})$  couplings remains relatively weak (0 to 50 Hz) and simple  $180^\circ$  pulses are sufficient for efficient decoupling. More complex decoupling schemes might be necessary according to the magnitude of  $^2\text{H}$ –X couplings, in particular for X nuclei with high values of  $\gamma$ .

Anisotropic samples of **1** (**2**) were prepared using 100 mg PBLG with a degree of polymerization of 534 (732), 100 (50) mg solute, and 350 mg  $\text{CHCl}_3$  in a tube of 5 mm o.d. (fire-sealed). Details concerning the preparation of anisotropic samples can be found in references.<sup>2,3</sup> The experiments were carried out at 303 K using a Bruker Avance HD spectrometer operating at 16.4 T equipped with an inverse  $^1\text{H}/^{13}\text{C}/^{15}\text{N}/^2\text{H}$  cryogenically cooled probe (107.5 MHz for  $^2\text{H}$ )<sup>17</sup> and including a z-axis gradient.

ADUF 2D spectra were recorded in a single-scan experiment. The following parameters were used for spatial encoding: a bipolar excitation gradient with gradients  $G_e$  of 20 ms and  $9.7 \text{ G cm}^{-1}$ , respectively, and smoothed chirp pulses of 20 ms with a sweep range of 5 kHz. The acquisition gradient parameters were  $T_a = 716.8 \mu\text{s}$  and  $G_a = 58.5 \text{ G cm}^{-1}$ . For samples **1** and **2**, the number of loops  $N_L$  was set to 256 and 128, respectively. The  $^2\text{H}$   $\pi/2$  pulse (87  $\mu\text{s}$ /38 W) was carefully calibrated to obtain an accurate  $90^\circ/180^\circ$  excitation. The spatial encoding and acquisition parameters resulted in a spectral width of 1000 Hz, which was sufficient to cover the spectral distribution of  $^2\text{H}$  information in both dimensions. The  $^1\text{H}$  and  $^{13}\text{C}$   $\pi$  pulses (21.3  $\mu\text{s}$ /180 W and 22.0  $\mu\text{s}$ /8.5 W, respectively) were also carefully calibrated to ensure optimal refocusing of heteronuclear couplings. Decoupling of  $^1\text{H}$  can be useful for removing possible residual  $^1\text{H}$ – $^2\text{H}$  couplings that are due to incomplete perdeuteration of molecules (in the case of **1**) or eliminating any long-range  $^1\text{H}$ – $^2\text{H}$  couplings in the case of selectively deuterated solutes (such as **2**).

All the ADUF 2D spectra were processed as follows: magnitude mode, zero-filling, Gaussian spatial apodization in the spatially encoded dimension  $F_2$ ,<sup>18</sup> and conventional sinebell apodization in  $F_1$  to obtain the most symmetrical  $^2\text{H}$  line shapes and find an optimal compromise between resolution and sensitivity. All the

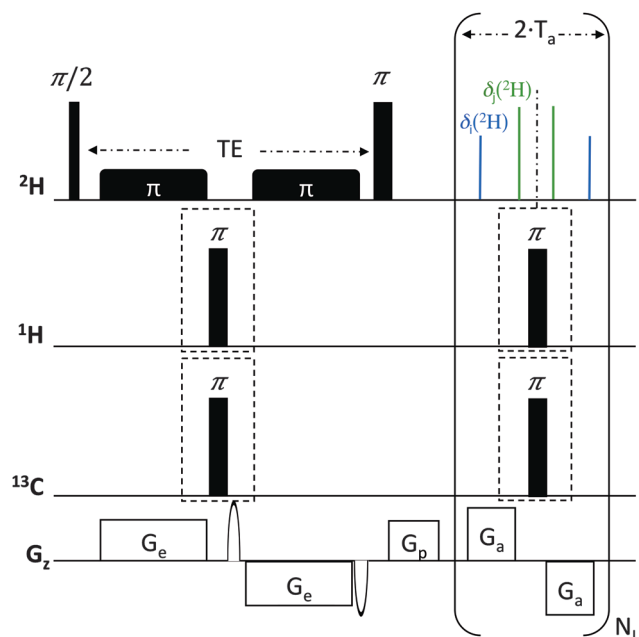


**Fig. 1** Pulse scheme of the ultrafast  $\delta$ -resolved constant-time NMR pulse sequence. The optional blocks for decoupling of  $^{13}\text{C}$  and  $^1\text{H}$  during the spatial encoding and acquisition periods are shown in dashed boxes. TE is the duration of spatial encoding.  $T_a$  is the duration of acquisition gradients.  $N_L$  is the number of loops applied in the EPSI scheme, which controls the resolution in the  $F_1$  dimension.  $G_e$  and  $G_a$  correspond to the gradients applied during spatial encoding and acquisition, respectively.  $G_p$  is a pre-acquisition gradient that is adjusted to center the peaks of interest in the middle of the spectral window. Additional sine-shaped gradients are used for the selection of coherence pathways.

spectra were analyzed using the Bruker program Topspin 3.2. The specific processing of ADUF spectra was performed using a home-written routine in Topspin. This processing program is available on a dedicated website, where a protocol is also provided to help users in the implementation of UF experiments.<sup>19</sup> The pulse sequence is available on demand. Other details are given in the figure captions.

As a first example, we investigated the case of 1-pentanol- $d_{12}$ . This prochiral flexible molecule of  $C_s$  symmetry possesses three homotopic C–D directions (from the methyl group) and four pairs of enantiotopic C–D directions, which are associated with the four prostereogenic methylenes of the molecule. *A priori*, nine QDs are expected to be detected if all inequivalent C–D directions are spectrally discriminated in the CLC, disregarding the hydroxyl group. The ADUF- $\{^1\text{H}\}$  2D spectrum recorded in a single scan is shown in Fig. 2, along with the corresponding projections. Note that all cases of  $\Delta\nu_Q(^2\text{H})$  have been eliminated in  $F_2$  and that no tilt is needed because this spatially encoded dimension is constant-time. The  $F_2$  dimension is therefore a “pure shift” dimension, which reduces the useful spectral information to  $\delta(^2\text{H})^{\text{aniso}}$  only (ca. 500 Hz of width).

This 2D map can be compared with a conventional anisotropic  $^2\text{H}$   $\delta$ -resolved 2D experiment recorded with 128 increments of  $t_1$  and eight scans in 17 min (see Fig. S1 and S2 in ESI†). Although the resolutions are lower than that of the conventional 2D map (or 1D spectrum), analysis of the ADUF spectrum shows that the discrimination of enantiotopic site pairs (which is visible for sites 1, 2 and 3) is similar to that observed on the conventional spectrum acquired in 17 min. However, the resolution in the  $F_1$  dimension of the ADUF spectrum ( $\Delta\nu_{1/2}(F_1) = 5.5$  Hz) is limited by the number of loops that the gradient amplifier can support in the EPSI block, whereas this resolution could be improved in the conventional spectrum by increasing the number of increments of  $t_1$ , although at the expense of time. The resolution in  $F_2$  ( $\Delta\nu_{1/2}(F_2) = 32$  Hz) is a well-known limitation in UF experiments, which is

inherent in the need to compromise between resolution, sensitivity and spectral widths.<sup>8</sup> Ultimately, the maximum spectral widths in  $F_2$  are limited by the maximum amplitude of the acquisition gradients  $G_a$ .

Nevertheless, these first results are very promising and clearly indicate that: (i) the detection of  $^2\text{H}$  nuclei by a UF approach within sub-second experimental times is possible for deuterated solutes; (ii) the gradient power ( $G_a$ : 40–60 G cm $^{-1}$ ) that is available on gradient units of routine spectrometers is sufficient to yield full-width 2D spectra in a single scan for nuclei with low gyromagnetic ratios – this would not have been possible at high field with  $^1\text{H}$  owing to the limitations in spectral width of UF NMR; and (iii) the resolution in  $F_1$  (a few Hz) allows the discrimination of enantiotopic sites down to differences in  $|\Delta\Delta\nu_Q|/2$  of <6 Hz.

To further examine the spectral possibilities of ADUF 2D experiments, we focused our attention on another solute of  $C_s$  symmetry, benzyl alcohol, which was isotopically enriched ( $^2\text{H}$  and  $^{13}\text{C}$ ) on the methylene group. Owing to the presence of abundant 100%  $^{13}\text{C}$  nuclei, four QDs (instead of two for the  $^2\text{H}$ – $^{13}\text{C}$  isotopologue) are observed on the  $^2\text{H}$ – $\{^1\text{H}\}$  1D spectrum (see Fig. S2, ESI†). The spectral difference between the two pairs of QDs corresponds to the difference in the total couplings of  $^2\text{H}$  and  $^{13}\text{C}$  ( $|^1T_{\text{C-D}}^{A,B}| = |^1J_{\text{C-D}}^{A,B} + 2^1D_{\text{C-D}}^{A,B}|$ ), which is associated with the enantiotopic directions pro-*R*/pro-*S* but is simply denoted as “A/B”. From the 1D spectrum several choices for pairing the components are possible, which lead to different values of  $|^1T_{\text{C-D}}^{A,B}|$ .

Fig. 3a presents the single-scan ADUF 2D  $\{^2\text{H}\}$  map of **2** in the PBLG mesophase that was recorded in 220 ms. In this second experiment, spectral resolutions of ca. 10 Hz ( $F_1$ ) and 32 Hz ( $F_2$ ) were reached; the lower resolution in  $F_1$  compared with Fig. 2 is explained by the lower number of EPSI loops. The two resonances observed in  $F_2$  are not associated with independent  $^2\text{H}$  peaks with distinct values of  $\delta(^2\text{H})$  (as for **1**) but originate from the total couplings,  $^1T_{\text{C-D}}^A$  and  $^1T_{\text{C-D}}^B$ , the resulting doublet being centered on the value of  $\delta(^2\text{H})^{A,B}$  of the methylene group. In contrast to homonuclear couplings, the evolution of the total heteronuclear  $^2\text{H}$ – $^{13}\text{C}$  couplings is not eliminated by constant-time

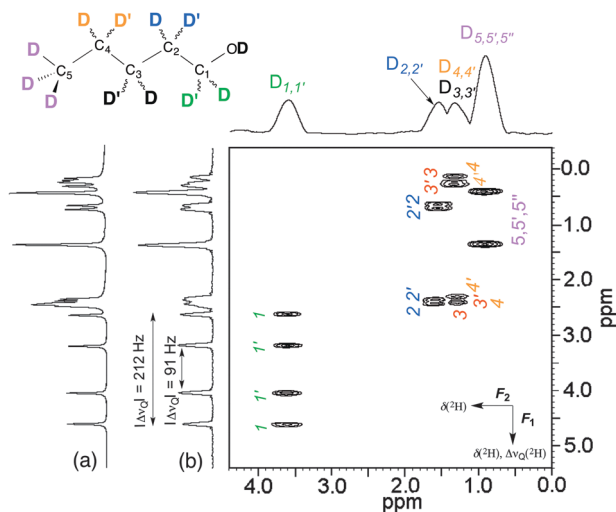


Fig. 2 (a)  $^2\text{H}$ – $\{^1\text{H}\}$  1D spectrum of **1** in a PBLG mesophase. (b) Single-scan ADUF- $\{^1\text{H}\}$  2D map recorded in ca. 400 ms with the pulse sequence of Fig. 1. The X/X' notation is arbitrarily defined.

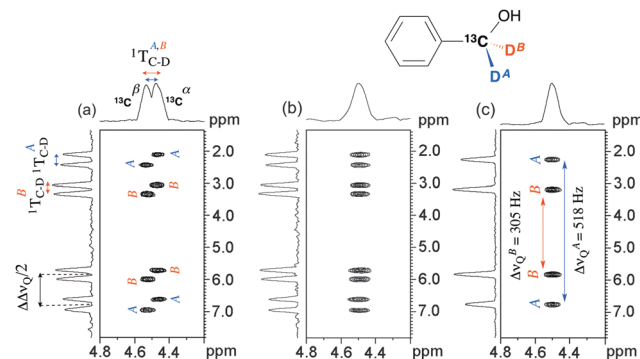


Fig. 3 Single-scan ADUF 2D  $^2\text{H}$ – $\{^1\text{H}\}$  maps of **2** in a PBLG mesophase without decoupling of  $^{13}\text{C}$  (a), with decoupling of  $^{13}\text{C}$  in  $F_2$  (b) and with decoupling of  $^{13}\text{C}$  in  $F_2$  and  $F_1$  (c), each of these recorded in ca. 220 ms. The A/B stereodescriptors shown on 2D maps are arbitrarily given. Note the increase in S/N ratios (by a factor of ca. 3) when the  $^{13}\text{C}$  signal is decoupled in both dimensions (map c).



chemical shift encoding. The presence of this doublet (which is due to the two energy levels of  $^{13}\text{C}$  nuclei ( $|\alpha\rangle$  and  $|\beta\rangle$ )) and the position of cross-peaks on the 2D map enable the two components of each QD pair (which are associated with the  $\text{C-D}^{A,B}$  directions) to be easily assigned and then the magnitudes of  $^1T_{\text{C-D}}^A$  and  $^1T_{\text{C-D}}^B$  determined to be equal to +29 and +35 Hz (on the 1D spectrum), respectively. Note that the moderate resolution in  $F_2$  leads to one doublet with broad components being detected instead of two resolved doublets.

Interestingly, the data contained on the ADUF 2D spectrum of **2** can be modulated according to the  $^{13}\text{C}$  decoupling blocks that were implemented in the TE and  $T_a$  periods of the initial pulse sequence (see Fig. 1). On the one hand, the decoupling of  $^{13}\text{C}$  during the spatial encoding collapses the doublet into a single resonance that is now centred on  $\delta(^2\text{H})^{\text{pro-R}} \approx \delta(^2\text{H})^{\text{pro-S}}$  ( $\text{CSA}(^2\text{H})^{\text{pro-R}} \approx \text{CSA}(^2\text{H})^{\text{pro-S}}$ ) in  $F_2$  (see Fig. 3b). On the other hand, the total  $^{13}\text{C}$ - $^2\text{H}$  coupling can also be eliminated by implementing  $^{13}\text{C}$   $180^\circ$  pulses between gradients in the EPSI block, which simplifies the spectral information to two QDs in  $F_1$ . Applying decoupling of  $^{13}\text{C}$  in both dimensions leads to the map shown in Fig. 3c, where the magnitudes of QD can be determined unambiguously ( $\Delta\nu_Q(^2\text{H})^A = +305$  Hz and  $\Delta\nu_Q(^2\text{H})^B = +518$  Hz). The positive sign is consistent with the values of  $^1T_{\text{C-D}}^{A,B}$  that were measured, considering that  $^1J_{\text{C-D}}^{A,B} = +22$  Hz (the ratio " $\Delta\nu_Q(^2\text{H})/^1J_{\text{C-D}}^{A,B}$ " = 70–80) for  $\text{sp}^3$  carbon atoms.

In the present work, we have demonstrated the experimental feasibility and analytical possibilities of anisotropic UF 2D NMR experiments in the case of quadrupolar nuclei such as deuterons. In practice, ADUF experiments are suitable for the study of weakly aligned deuterated solutes because the small magnitudes of  $\text{RQC}(^2\text{H})$  lead to a distribution of resonances over moderate spectral widths (< 1000 Hz), which is rather well adapted to the technical limitations of UF experiments. Consequently, these original experiments can be performed on routine NMR spectrometers equipped with basic gradient units when  $\gamma_{^1\text{H}}$  is 6.5 times less than  $\gamma_{^2\text{H}}$ . As has been shown, recording all the relevant anisotropic information of perdeuterated analytes is possible within sub-second experiment times, whereas the heteronuclear information (if detectable) can be modulated according to the decoupling scheme that is applied in both dimensions.

These pioneering findings open a vast array of prospects such as: (i) ADUF experiments in which the  $^2\text{H}$  chemical shifts would be refocused in the EPSI dimension ( $F_1$ ), similarly to Q-resolved 2D experiments;<sup>2</sup> (ii) the replacement of a constant-time scheme by a real-time scheme<sup>20</sup> to produce maps where the  $^2\text{H}$  autocorrelations would be distributed perpendicularly to the main diagonal, as in conventional  $^2\text{H}$  Q-COSY 2D maps; and (iii) the development of algorithms for processing UF spectra in phase-sensitive mode, thus improving the resolution. Although the samples studied in this paper were compatible with the acquisition of full-width spectra in a single scan, the sensitivity and spectral widths may be increased even further, if needed, by relying on hybrid experiments that have recently been described, which combine a few UF scans to improve the

analytical performance at a reasonable time cost.<sup>21</sup> Such hybrid experiments would also pave the way to the acquisition of fast 3D spectra to reduce peak overlap even further.<sup>22</sup>

There is no doubt that the ultimate challenge in ADUF experiments is sensitivity. Here, the sensitivity of a single-scan ADUF spectrum was found to be *ca.* six times lower than that of a single-scan 1D  $^2\text{H}$  spectrum. This is a well-known limitation of UF NMR.<sup>8</sup> Detailed measurements of SNR (see ESI†) show that the acquisition of a single-scan ADUF spectrum with our hardware requires at least 15 mg of  $^2\text{H}$ -labeled compound in the NMR tube. Although this limit of detection can be lowered by an order of magnitude by signal averaging, the detection of  $^2\text{H}$  nuclei at natural abundance levels<sup>4</sup> will require more sensitive techniques, such as hyperpolarization methods that can be efficiently coupled to UF 2D NMR.<sup>11</sup>

P. L. and P. B. thank the French CNRS and the Université de Paris-Sud for their recurrent funding of fundamental research.

## Notes and references

- (a) P. Lesot, *eMagRes*, 2013, **2**, 315; (b) C. Aroulanda, O. Lafon and P. Lesot, *J. Phys. Chem. B*, 2009, **113**, 10628; (c) K. Tabayashi and K. J. Akaska, *Liq. Cryst.*, 1999, **26**, 127.
- P. Lesot and J. Courtieu, *Prog. Nucl. Magn. Reson. Spectrosc.*, 2009, **55**, 128.
- (a) P. Lesot, C. Aroulanda, H. Zimmerman and Z. Luz, *Chem. Soc. Rev.*, 2015, **44**, 2330; (b) M. Sarfati, P. Lesot, D. Merlet and J. Courtieu, *Chem. Commun.*, 2000, 2069.
- (a) V. Baillif, R. J. Robins, S. Le Feunteun, P. Lesot and I. Billault, *J. Biol. Chem.*, 2009, **284**, 10783; (b) P. Berdagué, P. Lesot, J. Jacob, V.-J. Terwilliger and C. Lemilbeau, *Geochim. Cosmochim. Acta*, 2016, **173**, 337.
- M. Chan-Huot, P. Lesot, P. Pelupessy, L. Duma, G. Bodenhausen, P. Duchambon, M. D. Toney, U. V. Reddy and N. Suryaprakash, *Anal. Chem.*, 2013, **85**, 4694.
- (a) O. Lafon, B. Hu, J.-P. Amoureux and P. Lesot, *Chem. – Eur. J.*, 2011, **17**, 6716; (b) K. Kazimierzczuk, O. Lafon and P. Lesot, *Analyst*, 2014, **139**, 2702.
- L. Frydman, A. Lupulescu and T. Scherf, *J. Am. Chem. Soc.*, 2003, **125**, 9204.
- P. Giraudeau and L. Frydman, *Annu. Rev. Anal. Chem.*, 2014, **7**, 129.
- A. Herrera, E. Fernández-Valle, R. Martínez-Álvarez, D. Molero-Vilchez, Z. D. Pardo-Botero and E. Sáez-Barajas, *Magn. Reson. Chem.*, 2015, **53**, 952.
- L. H. K. Queiroz Jr, D. P. K. Queiroz, L. Dhooghe, A. G. Ferreira and P. Giraudeau, *Analyst*, 2012, **137**, 2357.
- J. N. Dumez, J. Milani, B. Vuichoud, A. Bornet, J. Lalande-Martin, I. Tea, M. Yon, M. Maucourt, C. Deborde, A. Moing, L. Frydman, G. Bodenhausen, S. Jannin and P. Giraudeau, *Analyst*, 2015, **140**, 5860.
- T. Jézéquel, C. Deborde, M. Maucourt, V. Zhendre, A. Moing and P. Giraudeau, *Metabolomics*, 2015, **11**, 1231.
- P. Giraudeau, T. Montag, B. Charrier and C. M. Thiele, *Magn. Reson. Chem.*, 2012, **50**, S53.
- P. Pelupessy, *J. Am. Chem. Soc.*, 2003, **125**, 12345.
- P. Mansfield, *Magn. Reson. Med.*, 1987, **1**, 370.
- D. Merlet, B. Ancian, J. Courtieu and P. Lesot, *J. Am. Chem. Soc.*, 1999, **121**, 5249.
- H. Kovacs, D. Moskau and M. Spraul, *Prog. NMR Spectrosc.*, 2005, **45**, 131.
- P. Giraudeau and S. Akoka, *Magn. Reson. Chem.*, 2011, **49**, 307.
- <http://www.univ-nantes.fr/giraudeau-p>.
- Y. Shrot, B. Shapira and L. Frydman, *J. Magn. Reson.*, 2004, **171**, 163.
- S. Akoka and P. Giraudeau, *Magn. Reson. Chem.*, 2015, **53**, 986.
- (a) R. Boisseau, B. Charrier, S. Massou, J. C. Portais, S. Akoka and P. Giraudeau, *Anal. Chem.*, 2013, **85**, 9751; (b) O. Lafon and P. Lesot, *Chem. Phys. Lett.*, 2005, **404**, 90.

